Science
AAAS

Supplementary Materials for

Title: Membrane proximal F-actin restricts local membrane protrusions and directs cell migration

Anjali Bisaria, Arnold Hayer, Damien Garbett, Daniel Cohen, and Tobias Meyer.

correspondence to: tom4003@med.cornell.edu, abisaria@stanford.edu

This PDF file includes:

Materials and Methods
Supplementary Text
Figs. S1 to S9
Captions for Movies S1 to S3
References (29-43)

Other Supplementary Materials for this manuscript includes the following:

Movies S1 to S3

Materials and Methods

Cell Culture

HeLa cells (ATCC CCL-2), HEK293T, hTERT-immortalized human umbilical vein endothelial cells (HT-HUVECs, described in (*30*)), hTERT-immortalized retinal pigment epithelial (RPE-1, ATCC CRL-4000), and rat mast cells (RBL-2H3) were used to create all cell lines. HeLa, HEK293T, and RBL-2H3 cells were maintained in DMEM (Thermo Fisher, 11995-065) supplemented with 10% FBS (Sigma-Aldrich, TMS-013-B). HT-HUVECs were maintained in EBM2 (LONZA CC-3156) supplemented with EGM2 (LONZA CC-4176). RPE-1s were maintained in DMEM-F12 (Life Technologies, 11039-047) supplemented with 10% FBS. Cells stably expressing fluorescent reporter constructs were created from RPE-1 or HT-HUVECs via lentiviral transduction followed antibiotics selection and/or FACs sorting. Cell sorting for this project was done on instruments in the Stanford Shared FACS Facility. Cells were passaged every 3-5 days to maintain sub-confluency.

Antibodies and reagents

Phalloidin conjugated to Alexa Fluor 568 (A12380), goat anti-Rabbit IgG conjugated to Alexa Fluor 647 (A-21245), Hoechst 33342 (H3570), and Opti-MEM (31985070) were from Thermo Fisher Scientific. CK-666 (SML0006), Bovine fibronectin (F1141), FITC-conjugated bovine collagen (C4361) were from Sigma-Aldrich. Y-27632 (13624) and Latrunculin A (ab428026) were from Cell Signaling Technologies (CST). Rabbit Anti-LIMK1 antibody was purchased from Atlas Antibodies (HPA025816). Limki 3 was from EMD Millipore (435930). SMIFH2 (4401) from Tocris, bFGF (223-FB) from R&D Systems, Latrunculin B (144291) from Abcam, Jasplakinolide (sc202191A) from Santa Cruz Biotechnologies, PLL-PEG (PLL(20)-g[3.5]-PEG(5)) from SuSos and Bovine collagen (PureCol - 5005-100ML) from Advanced BioMatrix were also used. Phalloidin conjugated to STAR 635P (ST635P-0100) was purchased from Abberior.

DNA constructs and lentivirus production

Selected plasmid constructs and corresponding sequence information will be available on Addgene soon after publication. (http://www.addgene.org/Tobias_Meyer). All constructs generated here used Gibson assembly into a Clontech backbone using a CMV promoter unless otherwise specified. Lentiviral backbones containing antibiotic resistance to neomycin, puromycin or blasticidin were created using pLenti-EF1a-MCS-IRES-antibiotic backbone (*30*). Lentiviral constructs were generated by digesting pLV plasmids with BamHI/EcoI and using Gibson assembly. Any g-blocks used were purchased from Integrated DNA Technologies (Coralville, Iowa) and were codon optimized for synthesis.

Control Constructs

#	Plasmid Name	Addgene #	Purpose	Source
1	C1-F-tractin-mCitrine		F-actin reporter	(*30*)
2	C1-F-tractin-mCherry		F-actin reporter	(*31*)
3	C1-F-tractin (Δ1-6) mCitrine		f-actin binding mutant of F-tractin	This study: Gibson, based off (*14*)
4	CFP-CaaX		Membrane Marker (farnesyl-polybasic membrane anchor)	(*13*)
5	YFP-CaaX		Membrane Marker (farnesyl-polybasic membrane anchor)	(*13*)
6	C1-iRFP-iLid-CaaX		Membrane Marker (farnesyl-polybasic anchor)	This Study: Gibson
7	C1-Lyn_{11}-CFP		Membrane Marker (Myristylation and palmitoylation anchor)	Gift from Mary Teruel
8	GFP-Moesin			gift of Bretscher Lab (*32*)
9	EZR(T567D)-GFP	20681	Constitutively Active from of Ezrin	gift from Stephen Shaw. (*33*)
10	CC-Rac1-Raichu		Codon Optimized YPet version of the Rac1-Raichu FRET sensor	Gift from the Matsuda Lab. Adapted from (*19*)
11	YFP-FKBP-Tiam1	20154	Rapamycin inducible global Rac1 activation	(*20*)
12	pCAG-Lyn_{11}-FRB		Membrane anchor for Rapamycin induced recruitment of FKBP constructs	(*20*)
13	FPC-1 myc LIMK1 CFP		Tagged Limk	Gift from Mizuno Lab (*9*)
14	YFP-SSH1L		Tagged SSH	Gift from Mizuno Lab (*9*)

MPAct Variants

#	Plasmid Name	Purpose	Source
15	C1-MPAct-mCitrine		1,4
16	C1-MPAct-mRuby3		1,4
17	C1-MPAct-mCherry		2,4
18	C1-MPAct(Δ1-6)-mRuby	F-actin binding mutant of MPAct	3,16
19	C1-MPAct-$EAAAR_8$-mCitrine	Increased linked length (~6 nm helical)	15, g-block for $EAAAR_8$
20	C1-MPAct-EEVEE-mCitrine	Increased linker length (flexible 120 A.A.)	15, 10 for EEVEE
21	C1-Lyn-mCitrine-EEVEE-LifeAct	MPAct variant exchanging both the membrane and f-actin binding domain	12,1, g-block for LifeAct
22	C1-mCit-FKBP-EZRabd(T567D)	Rapamycin inducible global recruitment of $Ezrin_{actin\ binding\ domain}$ (residues 552-586)	g-blocks, sequences derived from 1,9,11

Lentiviral Constructs

#	**Plasmid Name**	**Source**
23	pLV-iRFP-CaaX-IRES-Puro	
24	pLV-MPAct-mCitrine-IRES-Neo	15
25	pLV-MPAct-mRuby3-IRES-Puro	16
26	pLV-Turquoise-CaaX	
27	pLV-CC-Rac1-IRES-Blast	
28	pLV- PA-GFP-Actin P2A F-tractin-mRuby3-IRES-Neo	

Lentivirus was generated in HEK293T cells plated in 10 cm or 6 well collagen coated dishes. Prior to transfection, media was switched from DMEM+10% FBS to Opti-mem. Cells were co-transfected with the third-generation packaging plasmids pMDLg/pRRE, pRSV-rev, pCMV-VSVG (provided by X. Liu, University of Colorado, USA) using Lipofectamine 2000 (Life Technologies, 11668019) and a transfer vector containing the gene of interest. Viral supernatants were collected at 48-72 hours post transfection then filtered using .22 μm vacuum filters (Fisher Scientific, SCGP00525) and concentrated using centrifugal filter units (100 kDa cutoff, Millipore, UFC910024). Polybrene (EMD Millipore, TR-1003-G) was used at 10 μg/mL final concentration to increase lentiviral infection efficiency.

MPAct Reporter Design

The MPAct reporter is comprised of a fast-diffusing plasma membrane anchor that is linked to a fluorescent protein and a low-affinity F-actin binding domain (Fig. 1B). The rationale for the design was that this reporter could dynamically equilibrate along the surface of the plasma membrane and its concentration was expected to relatively increase in areas where there is more F-actin proximal to the membrane.

As a membrane anchor, we used a polybasic farnesylated CaaX motif derived from K-rasB (*13*), which localizes selectively to the inner leaflet of the plasma membrane and can diffuse quickly along the inner membrane leaflet (~1 $\mu m^2/s$) (*19*, *34*, *35*). Among different membrane anchored proteins tested, this CaaX motif also had a maximal diffusion coefficient and also showed a uniform surface membrane distribution at the resolution limit of light microscopy. The Lyn_{11} plasma membrane anchoring motif has a similar high diffusion coefficient but showed more internal membrane staining in some cell types which would complicate interpretation when using epifluorescence microscopy.

As an F-actin binding domain, we used a reversible F-actin binding domain from inositol 1,4,5-trisphosphate 3-kinase (F-tractin or FT) (*14*) which has been used as a live-cell F-actin marker (*30*, *36*, *37*). F-tractin has a low ~3 μM binding affinity for F-actin, and is less interfering than the F-actin markers Utrophin and LifeAct (*38*). The rapidly reversible binding of F-tractin to F-actin ensures that fast changes in MPA density can be monitored. The local diffusion coefficient of MPAct can be used as a proxy for the local density of MPA. An advantage of the relatively short anchor used in the MPAct reporter is that the diffusion coefficient is higher compared to that of longer linker proteins, which allows the MPAct to equilibrate rapidly. This would also allow for faster local MPA density changes to be monitored. Importantly, due to the limited search radius, MPAct

does not measure cortex thickness, but instead should only be able to sample the outer most shell of F-actin next to the plasma membrane.

Due to the fast diffusion of the MPAct reporter and the CaaX membrane marker along the inner membrane leaflet, ratiometric MPAct/CaaX signals reported the relative enrichment or depletion of MPA density in different membrane surface areas (Fig. 1C). Ratiometric comparison of the MPAct reporter to a membrane marker was critical for the analysis due to local submicroscopic invaginations and protrusions of membranes, and different x-y versus z resolution, that all could lead to apparent local MPAct intensity changes that instead reflect local changes in membrane topology. The MPAct value was generated by background subtracting each channel and then taking the ratio of the MPAct/CaaX channels. Ratiometric MPAct over CaaX intensities (here termed MPAct/CaaX or MPAct signals) can be used to measure relative local spatial heterogeneities in MPA density along the cell surface.

Advantages of using the specific synthetic MPAct reporter to monitor local MPA density changes and spatial MPA density gradients.

All membrane localized proteins with a reversible F-actin binding motif that we tested showed consistent back-to-front gradients, with the lowest signal in front during all forms of migration (Fig. S5B-E). This suggested that different reporter designs can in principle be used to measure local MPA density differences.

In initial studies, we considered whether ERM proteins themselves are suitable reporters of MPA density. At low expression levels we observed that WT GFP-Moesin is enriched in the rear of migrating cells (Fig. S6F-G) but there is a mix of cytoplasmic and membrane localized Moesin. In addition, Moesin is also known to be locally regulated by multiple signaling mechanisms and binds to F-actin with high affinity in its active form. Overexpression of constitutively active forms of ERMs, such as EZR_{T567D}, which actively anchor the plasma membrane to the actin cortex ,can change membrane tension (*39*) and are therefore less useful as potential MPA density reporters. Another argument against using an ERM or similar protein as a MPA reporter is that MPA density is regulated by additional mechanisms such as Arp2/3 and formin-mediated actin polymerization, cofilin-mediated severing of F-actin, and alternative F-actin-membrane linker proteins (e.g. EBP50 or E3KARP) (*40*) that may not be captured when using the localization of ERM proteins alone as a proxy for MPA density. ERM derived constructs are not ideal reporters for MPA density due to their high F-actin binding affinity, their partitioning to the cytoplasm, and their locally regulated binding interaction with the membrane and F-actin.

Immunofluorescence, Phalloidin, and Fixed Imaging

Cells were sparsely (2.5×10^3/well) plated in a collagen coated 96-well plate (Cellvis, P96-1.5H-N) and allowed to adhere overnight. Cells were fixed with 4% paraformaldehyde. After 15 min the solution was washed 3x in PBS followed by 15 min of a pre-permeabilization buffer (0.2% Triton in PBS), and 60 min incubation with a combined permeabilization/ blocking solution (0.1% Triton X-100, 10% FBS, 1% BSA, 0.01% NaN_3, in PBS, called BB). Primary Limk antibodies (1:1000) were incubated overnight at 4˚C in BB, washed 3x in PBS and secondaries (1:2500 in BB) were left for 1 hour at RT. Phalloidin was diluted into BB (1:200 FITC-phalloidin, 1:50 647-phalloidin)

and incubated for 1 hour at RT with secondary. For applicable experiments, cells were stained with Hoechst (1:10,000) for 10 min at RT then washed 3x with PBS. For images shown in Fig S2B (MPAct), S9J(mCherry), cells were transiently transfected with fluorescent reporters as indicated and the fluorescent proteins were imaged post-fixation in the appropriate wavelength.

Live-cell imaging

Unless otherwise specified, all migration assays were performed on 96 well glass-bottom plates (Cellvis, P96-1.5H-N) pretreated with 31 μg ml^{-1} bovine collagen (Advanced BioMatrix, 5005-B) in PBS at 37 °C for at least 30 min. For 1D migration assays cells were plated on micropatterned ibiTreat 35 mm dishes as described below. Live cells were imaged in EGM2 buffered with 20 mM HEPES pH 7.4 or extracellular buffer (ECB, 125 mM NaCl, 5 mM KCl, 1.5 mM $MgCl_2$, 1.5 mM $CaCl_2$, 10 mM D-glucose supplemented with 1% FBS and 5 ng ml^{-1} bFGF). 96-well plates were kept sealed during long term imaging using PolarSeal Foil Sealing Tape (E & K Scientific, T592100).

Images from Fig. S3J were acquired on a Leica DMi8 S with Infinity TIRF equipped with 488 nm and 561 nm lasers and a 100x Plan Apo objective. 96 well plates were environmentally controlled using an Okolab stage top incubator (H301-K-Frame).

All other images shown were acquired using a fully automated widefield/Yokogawa spinning-disc confocal fluorescence microscope system (Intelligent Imaging Innovations, 3i), with a Nikon Ti-E stand, equipped with Nikon 40× 1.3NA oil, 60× 1.27 NA water-immersion and 100x 1.4 NA oil objectives, an Olympus 60× 1.35 NA oil immersion objective, a 3i laser stack (405, 442, 488, 514, 561, 640 nm), a 3i 'Vector' photomanipulation device, an epifluorescence light source, (Sutter Lambda XL), a Yokogawa CSU-W1 scanning head with dual camera port, two sCMOS cameras (Andor Zyla 4.2), enclosed by an environmental chamber (Haison), and controlled by SlideBook 6.0 software (3i). FRET data was acquired with a CFP/YFP dichroic and two cameras enabling simultaneous acquisition of CFP/FRET signals.

For experiments with drug additions, drugs were added as a 2x solution in ECB unless otherwise specified. Time is reported to relative to the addition of the drug to the media. For a list of imaging conditions for each Figure/analysis please see the table below:

Microscope	3i Nikon Ti-E				Leica
Settings	Epi	Confocal			TIRF
	40x	40x	60x	100x	100x
Figs.	2A-D; 3C-D	3A-B, E-L 4; 5D	1C-D; 2E, 5A-C, E-H	1E	
Supp. Figs	S3B-E, I; S4G-K; S7A-B	S2C;S4A,D-F,L; S6D-F; S7C-J; S8B, S9B,M	S1B-F; S2A-B, D-E; S3H; S4B-C; S5; S6B-D, G; S8D-F; S9C-K,N-O		S3J

Transient transfections of DNA

For transient transfection of DNA, 1-5 × 10^3 cells per well were plated the day before transfection in glass-bottom 96-well plates coated with collagen as described above. On the day of transfection, 0.1 - 0.2 µg DNA of each construct (unless noted otherwise) and 0.25 µL Lipofectamine2000 diluted in 20-40 µL OptiMEM, were added following the manufacturer's protocol. For HT-HUVEC cells, the OptiMEM mixture was added to growth media up to a total volume of 100 µL. For all other cell types growth media was replaced with OptiMEM to a final volume of 100 µL. This transfection mix was replaced after 2-4 h with growth media and cells were imaged 16–24 h later.

Fibronectin Micropatterning for Linear Tracks

Fibronectin stamping was adapted from (*41*). Briefly, 20 µm linear tracks were generated creating a PDMS (Sylgard Silicone Elastomer Kit 184, Ellsworth #4019862) stamp from an SU8 pattern. PDMS was cured for at least 3 hours at 65° C and then cut into smaller stamps (~0.5 cm^2) using a scalpel. 40 µL of 50 µg/mL fibronectin was spread onto the stamp and incubated at 37° C for at least 30 min. Stamps were washed 3x with 50 µl ddH_2O and then left to air dry for ~15 min until stamps were completely dry. Stamps were then placed onto plasma cleaned Ibidi µ-Dish 35 mm, high dishes (Ibidi, 81156, plasma treated for 30 seconds at 250 mTorr) using forceps. Stamps were then removed and incubated with 500 µL of 1 mg/mL PLL-PEG and 10 mM HEPES in ddH_2O for 30 min at 37° C. Plates were washed 3x with 750 µL PBS and stored in PBS until use, usually within 1-2 weeks.

3D collagen gel migration

Glass bottom 96-well plates were plasma cleaned for 30 seconds at 250 mTorr. All collagen handling steps were performed on ice or with ice cold reagents. PureCol was diluted to a concentration of 2.4 mg/mL into 10x PBS pH 7.5. pH was adjusted to be 7.5 before further dilution into cold 1X PBS for a final concentration of 0.5 mg/mL. 60 µL of the collagen solution was added to the bottom of the well and allowed to polymerize for 2 hours at 37° C. The gel was washed with PBS 5x, always keeping the gel covered with some aqueous solution. 50 µL of RPE-1 cells at a concentration of 2 × 10^4 cells/mL were added to each well and allowed to settle for 2-3 hours before removing 40 µL of media and adding an additional 60 µL of collagen on top the cells. Wells were washed with growth media 6X and put back in a 37° C incubator. Cells were imaged after 24 hours. Before imaging growth media was exchanged for ECB.

JLY/JYB experiments

JLY actin-arresting experiments were performed according to the protocol described in (*42*). Briefly, cells were pre-imaged in ECB, then incubated in 20 µM Y27632 for 10 min before the addition of 8 µM jasplakinolide and 5 µM latrunculin B. For the JBY cocktail, 100 uL of a 2x solution was added to cells for a final concentration of 8µM jasplakinolide, 20 µM Y-27632, and 10µM blebbistatin.

Lateral Diffusion FRAP acquisition and analysis

For lateral diffusion calculations (Figs. 1D, S1D, F, S4C) HeLa or RPE-1 cells were transiently transfected with plasmids expressing FT-mCitrine, MPAct-mCitrine, mCitrine-CaaX or CFP-CaaX driven by a CMV promoter. Before imaging growth media was exchanged for ECB.

Confocal images of midsection of the cells were taken using a 60x oil objective. A 2 µm circle of lateral membrane was photobleached using consistent laser power (usually between 2-5% of total output). Identical bleaching parameters were used across experiments taken on the same day. The spot that was bleached remained in the same location for each acquisition. For Figure S1B images were acquired every second. For other acquisitions images were taken at different frequencies over time (5×1s, 5×0.5s, 5×1s, 10×3x, 2-3×10s) to allow for proper fitting of the initial lateral diffusion rate. Photobleaching always occurred after the 5th frame (5 seconds).

For each FRAP curve, the membrane area was selected in MATLAB by hand using IMROI and then automatically segmented to mask out any background areas. The pixels in the region were background subtracted, bleach corrected based on the first 5 frames, and divided by the initial fluorescence intensities in that region. All FRAP recoveries were fit in GraphPad Prism using a one phase association.

For lateral diffusion rates, the membrane region was auto-rotated such that the axis along the membrane was horizontal. Then the average value for each x-pixel was generated for each time point. The recovery of this area was fit to a 3D surface in MATLAB using cfit and the equation

$$F(x,t) = 1 - B \times \frac{r_o}{\sqrt{4Dt + r_o^2}} \times e^{-\frac{(x-c)}{4Dt+r_o^2}}$$

Where x is the distance in µm, t is time in seconds. This equation was used to explicitly solve for the following parameters: r_o - initial bleach radius, c - offset of the bleach spot from 0, and D - diffusion coefficient in $\mu m^2/s$. Rates were fit using the first 5 time points after recovery (0.5 s each for 2.5 seconds).

Kymograph of fluorescent proteins in blebs

Pixel intensities were measured using the plot profile function in FIJI with a linewidth of 11 px (~ 2 µm). Resulting values were then plotted in MATLAB using the imagesc function.

2D FRAP acquisition and analysis

To compare recovery rates of expressed constructs in the front and back of polarized cells, HT-HUVEC or RPE-1 expressing a fluorescent protein were plated on either a fibronectin stripes as described above or collagen coated glass bottom plate. Cells were monitored to make sure they were actively migrating and polarized. Images were taken at different frequencies over time (5 x 1s, 5x 0.5s, 5x 1s, 10x 3x, 2-3x10s). A 5 µm circle was photobleached in both the front and back of each cell, alternating between front or back being bleached first. The same ROI within the field of view was used for all experiments to control for alignment of the laser.

For analysis, a mask was generated using the average difference between all the frames before and after photobleaching acquisitions from the same day. The average

value in the mask was calculated after background subtraction, bleach correction, and initial value normalization based on the first 5 frames. The fits shown were performed in GraphPad Prism using a one phase association. The individual $T_{1/2}$ shown in Fig.S4H-I, S6C are derived from those individual fits.

Cell tracking and motility analysis.

Segmentation of membrane and cell tracking were adapted from previously designed MATLAB scripts (*30*). Masks of individual cells were identified using a modified Otsu's method or the adapthresh function in MATLAB on the CaaX or membrane localized fluorescent protein. Cells that were not fully enclosed in the frame were excluded. Nearest-neighbor heuristics between subsequent frames was used to track cells. Cell velocity was determined on the basis of centroid displacements between subsequent time points (15 s- 3 min) averaged over 3 time points. Cell direction was determined by fitting the trajectory of the cell's XY location to a first order polynomial and then extrapolating the direction of the cell to minimize the effects of random centroid movements.

Sensor activity profiles in 1D migrating cells

For HT-HUVEC, MPAct-mCitrine and CFP-CaaX or MPAct-mRuby and Rac1-Raichu FRET sensor were stably expressed. Cells were plated at 2-3 × 10^3 cells per 6-well Ibidi dish and imaged 24 hours later. Time-lapse imaging of polarized and unpolarized cells was acquired using a 40× 1.3NA objective (0.325 μm pixel resolution), at 30 s - 4 min intervals. Cells were tracked over at least 60 min based on using the CaaX or Rac channel.

For each cell mask, a 3 μm ring was created around the periphery for each time point. The ring was then divided into 20 equally distributed segments along the front-back axis of the cell for better comparisons between cells. Each value of the normalized biosensor intensity in the ring mask was binned into one of the 20 segments based on its distance to the cell front thus creating the kymograph for each time point. For all sensor activity kymographs time is shown on the x axis, and each of the 20 spatial bins into a single line with front/back annotated on the graph.

For 1D correlation scores, at each timepoint the 1D distribution (1x20 value) of CaaX was correlated with the 1D distribution of MPAct and MPAct(Δ1-6) to create a corresponding correlation value (between -1 and 1).

Polarity Score and Average Speed

The polarity score was determined from activity sensor profiles in migrating cells. Average polarity was calculated by using the absolute value of (mean(front 10%) – mean(back 10%)). All cells were tracked for at least 60 min with a 1-2 min imaging interval. Average speed was calculated using centroid displacement over the time tracked.

Edge velocity and biosensor spatial activity maps

Analysis was adapted from (*18*). Briefly, time-lapse sequences were acquired at 15 s - 2 min intervals, using a 40× 1.3 NA objective or 60x 1.27 NA objective. The cell body was defined based on a membrane signal (either CaaX or the YFP of the Rac1-Raichu

FRET biosensor). For each frame, 120 markers were equally spaced along the cell boundary and shifted to minimize the median distance from the markers in the previous frame. This method enabled continuous tracking of markers and uniform spatial sampling of the cell edge. The average value of either the individual biosensor or a ratio signal (for MPAct/CaaX, Rac1 FRET) was calculated for each window such that the edge velocity and the sensor activity or distribution could be compared. A negative window edge velocity represents a retraction toward the cell body whereas a positive value represents a protrusion away from the cell body. For all edge velocity kymographs time is shown on the x-axis, and each of the 120 windows is arrayed into a single line where window 1 and window 120 are adjacent. The windows are numbered such that they are always the same orientation with respect to field of view (e.g. if a cell moves at a constant angle, the protrusive region will show a high edge velocity within the same windows over time).

Line-scan of MPAct and Protrusion Length

For the graphs in Fig. 3G-I the normalized MPAct/CaaX ratio was generated after background subtraction and bleach correction of the individual channels in FIJI. A line segment shown in Fig. 3G (left, red line) was used to measure the intensity of the ratio with the plot profile function (shown in Fig. 3H). The maximum value of each profile was used for Fig. 3I. A mask of the cell was generated using thresholding of the CaaX channel and the protrusion length was determined by the overlap of the line segment with the mask.

Protrusion and MPAct Alignment

For all experiments, RPE-1 cells were plated sparsely on collagen coated 96-well glass bottom plates and analyzed with edge-correlation analysis scripts. Cells that showed a distinct repolarization based on edge velocity profiles were selected. The spatial region associated with the repolarization was automatically selected by thresholding for the top 20% of protrusion values and using the window numbers that are contained in that region. Once this region was selected, the corresponding MPAct values in that same region and time were used for comparison. MPAct values are normalized to be between -0.5 and 0.5 to allow for direct comparison between cells with different shapes and expression levels. The time average edge velocity was taken for this region to find the moment where the average velocity first became greater than 0 μm/s. This became the zero-point for protrusion and all average traces were aligned to this value. To be included in the final analysis, repolarization events had to have at least 10 min of tracking before and after the repolarization event.

Rac1, Edge Velocity, & MPAct Alignment

RPE-1 cells co-expressing the Rac1 FRET sensor and MPAct-mRuby were acquired using simultaneous confocal imaging. Areas of abrupt increase in Rac1 signaling automatically detected by segmenting areas of high Rac1 activity (normalized value > 1.1) next to areas that were lower. The corresponding average Rac1, edge velocity and MPAct values were taken in those areas in a window of 10 min before and after the beginning of the Rac1 patch. All three average traces values were in silico aligned to time of ½-maximal activation of Rac1.

Tiam1 Edge velocity after Global Rac Activation

2-3 × 10^3 HeLa were plated on collagen coated 96-well plates and then transfected 24 hours later with 100 ng of iRFP-CaaX and MPAct-mRuby, 270 ng Lyn-FRB, and 30 ng YFP-FKBP-Tiam1 (both described in (*20*)) using .25 µL of lipofectamine in 20 µL of OptiMEM for each well. Media was changed after 2 hours and cells were imaged 24 hours later. Prior to imaging, growth media was exchanged for ECB. We found translocation was more robust when there were higher levels of Lyn-FRB expressed than FKBP construct. Translocation was induced by adding 100 µL of a 2x Rapamycin solution (500 nM) diluted into ECB. Cells were tracked, and edge velocity analysis run as described above. The regions of highest and lowest MPAct was calculated based on a 5% moving average (6 windows) of the MPAct values prior to rapamycin addition. The average edge velocity for these windows were compared for each cell over time.

Hypo-osmotic Shock and maximal edge extension

1-2 × 10^3 RPE-1 were plated on collagen coated 96-well plates and transiently transfected as described above with 100 ng of F-tractin-mCherry, 100 ng of MPAct-mCitrine, and 100 ng of CFP-CaaX. Prior to imaging, media was exchanged for ECB. Cells were imaged for every 20 sec, 10 min before addition of 100 uL of ddH_2O, and then monitored for another 10 min. Cells were automatically segmented and tracked based on the CFP-CaaX channel as described above and extension analysis was performed as follows: For each cell a 10-pixel area with low and high MPAct/CaaX were selected based on the timepoint prior to ddH2O addition. Then the average minimum distance of each of those points to the perimeter of maximal cell mask of all timepoints after hypoosmotic shock was calculated. Here we use the minimum distance to conservatively measure how far that local region could have protruded after the osmotic shock.

$Ezrin_{abd}$ Retraction Analysis

1-2 × 10^3 RPE-1 were plated on collagen coated 96-well plates and transiently transfected as described above with 100 ng of F-tractin-mCherry, 100 ng Lyn-FRB, and 100 ng of either YFP-FKBP (described in (*20*)) or mCitrine-FKBP-$EZR_{ABDT567D}$. mCitrine-FKBP-$EZR_{abdT567D}$ contains the actin binding domain (a.a. 549 – 586) of the constitutively active form of Ezrin (T567D). Before imaging media was exchanged for ECB. Cells were pre-imaged for 5 min prior to addition of 100 µL of 10 µM Rapamycin for a final concentration of 5 µM. For analysis, only cells that (1) showed visible translocation of the FKBP construct and (2) had an active protrusion at the time of translocation were considered for analysis. The fraction presented in 4H represents the # of retraction events/ (# of cells with active protrusions and # of cells with FKBP translocation) for both control and EZR_{ABD} constructs.

PA-GFP-Actin turnover

RPE-1 were stably infected with PA-GFP-Actin P2A F-tractin-mRuby3 and selected with Neomycin for 1 week. 1-2 × 10^3 cells were plated on collagen coated 96-well plates and allowed to settle overnight. Prior to imaging, media was exchanged for ECB. For all cells, a line was bleached along the axis of migration for the cell after the first image using a 445 nm laser at 10% power. Images were taken at a 2 s interval. For quantification, ROIs that included the front and back part of the cells were manually

outlined in FIJI along with similarly sized, adjacent background regions. To create the turnover curves the adjacent background region was subtracted for each time point and then the entire curve was max normalized to 1. For drug additions migrating cells were selected prior to drug addition and imaged within 10 min of addition to capture fast F-actin turnover changes.

Mean MPAct in cells after JYB addition

1-2 × 10^3 RPE-1 were plated on collagen coated 96-well plates and transiently transfected with MPAct-mRuby3. Prior to imaging, media was exchanged for ECB. Front and back area was selected and measured using FIJI ROI multi measure plugin. Values were normalized by dividing by the 5 frames prior (20 sec. interval).

Protrusion Area Change after Limki 3 addition

1-2 × 10^3 RPE-1 were plated on collagen coated 96-well plates and transiently transfected as described above with 100 ng of F-tractin-mCherry, MPAct-mCitrine, and CFP-CaaX per well. Prior to imaging, media was exchanged for ECB. Protrusive area was measured using FIJI at the frame prior and 5 min after 20 μM Limki or DMSO treatment. The protrusion area was defined by the area that was actively protruding before drug addition that also had low MPAct.

MPAct/CaaX and SSH/Limk intensity after Limki 3 addition

1-2 × 10^3 RPE-1 were plated on collagen coated 96-well plates and transiently transfected as described above with 100 ng of LIMK1-CFP, YFP-SSH1L, MPAct-mRuby3, and iRFP-CaaX. Prior to imaging, media was exchanged for ECB. Images were background subtracted and then ratioed in FIJI before using the ROI manager to calculate the average intensity in regions selected in the front and back.

Supplementary Text

Experimental validation that the MPAct reporter can bind membrane proximal F-actin

Using FRAP of the lateral membrane of HeLa, CaaX alone showed an apparent diffusion coefficient of 0.96 ± .05 (95% CI) $\mu m^2/s$, similar to previously reported values (Fig. 1E). The diffusion of MPAct was slower under normal conditions (0.30 ± .03 (95% CI) $\mu m^2/s$), but this difference was abolished after addition of 1 μM LatA (0.88 ± .10 (95% CI) $\mu m^2/s$). Confocal imaging of RPE-1 cells transiently co-transfected with fluorescently labeled CaaX, MPAct, and F-tractin revealed that the MPAct reporter is exclusively localized to the plasma membrane but has a different distribution from the plasma membrane marker CaaX alone (Fig. 1F). Furthermore, while some regions with high F-tractin concentration also had high MPAct intensity (Fig. 1F, arrows), other regions had both high F-tractin and CaaX intensities but low relative MPAct intensity (Fig 1F. arrowhead). This suggests that some regions in a cell can simultaneously have a high regional F-actin density (~250 nm scale of the microscope resolution) but a low F-actin density proximal to the plasma membrane (less than 10 nm scale based on linker length) (Fig. 1F, arrowhead in merged and MPAct/CaaX image). Similar relative local distributions were observed in HeLa cells (Fig. S2A).

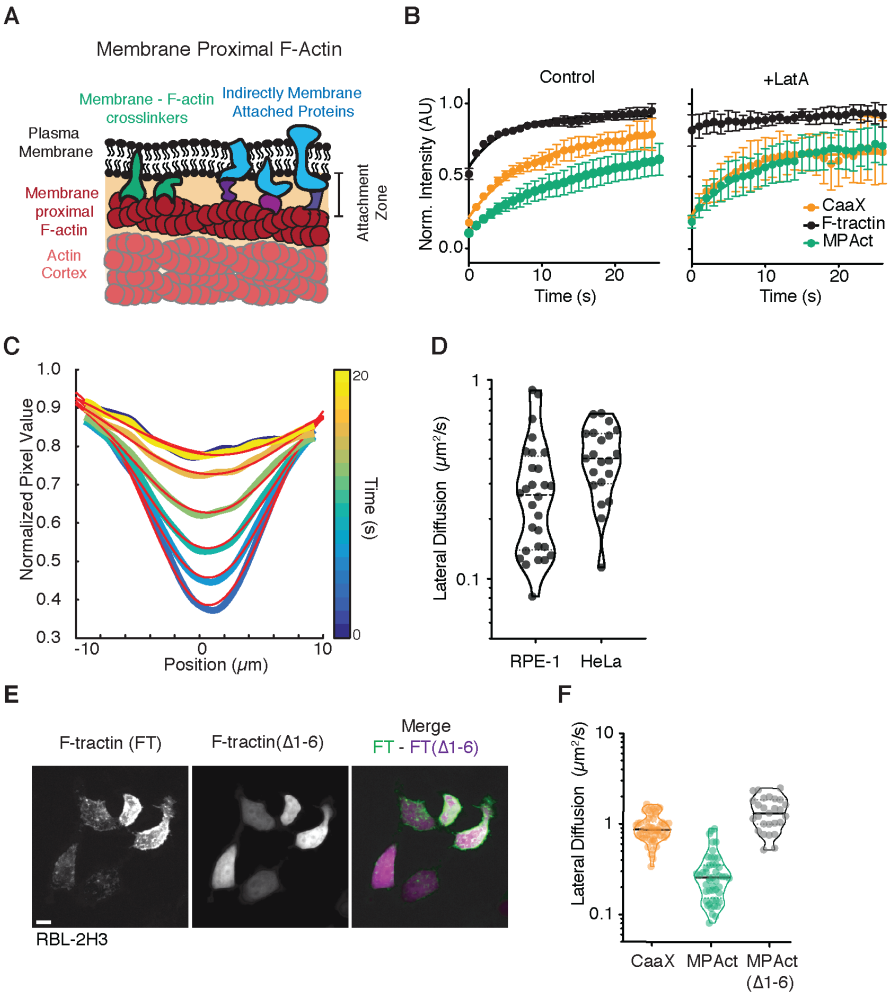
A
Membrane Proximal F-Actin
Membrane - F-actin crosslinkers
Indirectly Membrane Attached Proteins
Plasma Membrane
Membrane proximal F-actin
Actin Cortex
Attachment Zone
B
Control
+LatA
Norm. Intensity (AU)
Time (s)
CaaX
F-tractin
MPAct
C
Normalized Pixel Value
Position (μm)
Time (s)
D
Lateral Diffusion (μm²/s)
RPE-1
HeLa
E
F-tractin (FT)
F-tractin(Δ1-6)
Merge
FT - FT(Δ1-6)
RBL-2H3
F
Lateral Diffusion (μm²/s)
CaaX
MPAct
MPAct (Δ1-6)

Fig. S1 Diffusion of the MPAct reporter is slowed by binding MPA.

(**A**) Schematic showing F-actin close to the membrane in an "attachment zone" where different linker mechanisms can attach the membrane to membrane proximal F-actin (MPA). MPA is only a small part of a much thicker F-actin cell cortex. (**B**) FRAP analysis in HeLa transiently expressing F-tractin-mCitrine (Black), YFP-CaaX (Orange), or MPAct-mCitrine (Green) under control conditions (left) or after treatment with 1 μM of Latrunculin A (LatA, right). As expected, cytosolic F-tractin showed a rapid recovery due to its low affinity F-actin binding (Fig. S1A, black line $t_{½}$ = 2.32 ± 0.38 s) under untreated conditions. The CaaX construct showed slower recovery due to its 2D confined diffusion along the plasma membrane. Consistent with having an additional F-actin binding interaction, the recovery rate of MPAct was slower than that of the CaaX marker ($t_{½}$ = 5.50 ± 0.97s and 9.54 ± 2.70 s respectively). We confirmed that the slower rate was dependent on F-actin by addition of 1 μm Latrunculin A (LatA), a potent F-actin inhibitor, which resulted in a nearly identical recovery rate of the MPAct reporter and the CaaX membrane marker ($t_{½}$ = 3.31 ± 1.01s and 4.51 ± 1.60 s respectively).
Cells were monitored over 30 seconds. n ≥ 6 cells for all conditions. Error bars are 95% confidence intervals (CI) $T_{½}$.values are reported as mean ± 95% CI. (**C**) Fitting of a single FRAP curve of CFP-CaaX to calculate observed diffusion coefficients using a widening gaussian diffusion profile (*35*). Position along the membrane (±10 μm) is shown in the x-axis with intensity on the y-axis. Time is shown in a parula colormap with corresponding line of best fit overlaid in red. (**D**) Reproducibility in MPAct lateral diffusion between cell types. Lateral diffusion rates in the membrane were calculated in unpolarized HeLa (N = 20 cells) and RPE-1 (N = 28 cells). (**E**) Max projection of RBL2H3 transiently co-expressing F-tractin-mCherry (left), F-tractin(Δ1-6)-mCitrine (middle) (*14*). The deletion of these 6 amino acids was previously shown to abolish F-actin binding affinity. (**F**) A mutant MPAct deficient in binding F-actin (MPAct(Δ1-6)) was created by removing the first 6 amino acids from MPAct, corresponding to the same 6 amino acids deleted in (E). Diffusion rates calculated from FRAP experiments preformed on the lateral membrane of RPE-1 based on 3D Gaussian profile fitting for CFP-CaaX, MPAct-mCitrine, and MPAct(Δ1-6)-mCitrine. N =51,48, and 27 cells respectively, pooled from 2 independent experiments. CFP-CaaX and MPAct-mCitrine data are identical to Fig 1D.

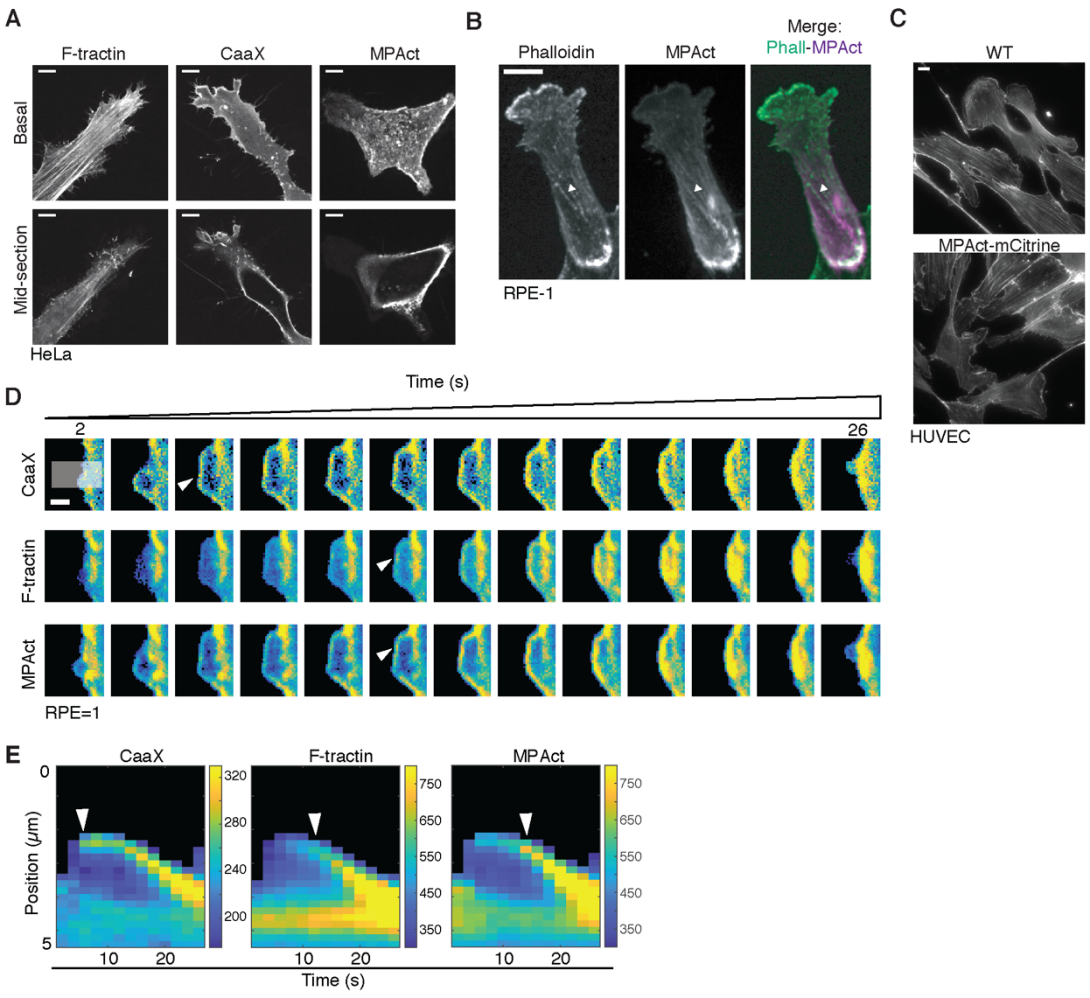
A
F-tractin
CaaX
MPAct
Basal
Mid-section
HeLa
B
Phalloidin
MPAct
Merge:
Phall-MPAct
RPE-1
C
WT
MPAct-mCitrine
HUVEC
D
Time (s)
2
26
CaaX
F-tractin
MPAct
RPE=1
E
CaaX
F-tractin
MPAct
Position (μm)
0
5
10
20
320
280
240
200
750
650
550
450
350
Time (s)

Fig. S2 The MPAct reporter is localized to the plasma membrane and is enriched in surface membrane areas with higher MPA

(**A**) Confocal slices of HeLa transiently transfected with F-tractin-mCitrine (left),YFP-CaaX (middle), and MPAct-mCitrine (right). Basal (top) and mid-plane (bottom) are shown. (**B**) RPE-1 cells transiently expressing MPAct-mCitrine were fixed and stained with phalloidin. Some MPAct fibers were also marked by phalloidin (arrowhead). These distributions are consistent with the reporter binding only to a subset of F-actin that is close to the plasma membrane within the linker length. (**C**) WT (top) and MPAct-mCitrine (bottom) expressing HT-HUVEC fixed and stained with phalloidin-568. Expression of the MPAct reporter does not cause observable changes in overall F-actin organization. (**D**) Time series of CFP-CaaX (top), F-tractin-mRuby3 (middle), and MPAct-mCitrine (low) during a bleb life cycle in RPE-1 cells. Upon membrane detachment, expanding blebs are initially devoid of contractile F-actin cortex. MPAct remains localized to the PM and enriches at the same time and location as F-tractin within the bleb. Only after de novo polymerization of a new cortex, does the bleb retract. MPAct showed preferential accumulation where both membrane and F-actin are located during the rapid lifecycle of blebs. This sets a baseline for the spatiotemporal resolution of the sensor. Scale bar = 2 μm. Boxed region is analyzed as kymographs in (E). (**E**) Individual channel kymographs from region highlighted in (D) for CFP-CaaX (left), F-tractin-mCherry (middle) and MPAct-mCitrine (right). Arrowheads denote time where signal is first enriched. Images in (D) are shown with the same colorscale in (E). Images taken every 2 seconds (horizontal axis). For all images scale bar = 10 μm unless otherwise noted.

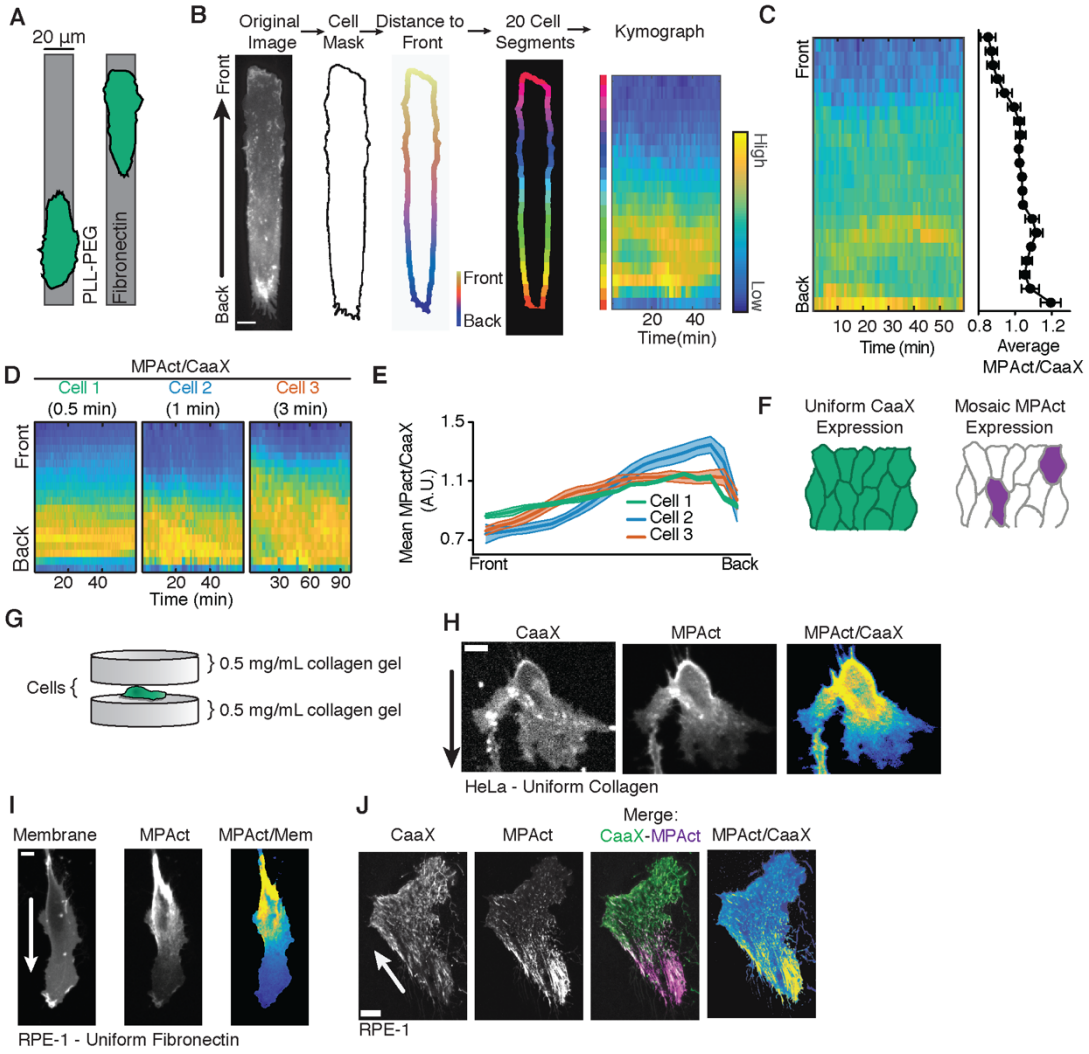
A
20 µm
PLL-PEG
Fibronectin
B
Original Image
Cell Mask
Distance to Front
20 Cell Segments
Kymograph
Front
Back
High
Low
20 40
Time(min)
C
Front
Back
10 20 30 40 50
Time (min)
0.8 1.0 1.2
Average MPAct/CaaX
D
MPAct/CaaX
Cell 1 (0.5 min)
Cell 2 (1 min)
Cell 3 (3 min)
Front
Back
20 40
20 40
30 60 90
Time (min)
E
Mean MPact/CaaX (A.U.)
1.5
1.1
0.7
Cell 1
Cell 2
Cell 3
Front
Back
F
Uniform CaaX Expression
Mosaic MPAct Expression
G
Cells {
} 0.5 mg/mL collagen gel
} 0.5 mg/mL collagen gel
H
CaaX
MPAct
MPAct/CaaX
HeLa - Uniform Collagen
I
Membrane
MPAct
MPAct/Mem
RPE-1 - Uniform Fibronectin
J
CaaX
MPAct
Merge:
CaaX-MPAct
MPAct/CaaX
RPE-1

Fig. S3 Gradients of MPAct signals with low MPAct signals in the front during migration can be observed in different cells types and migration modes, and using different types of microscopy analysis

(**A**) To facilitate measurements of potential MPA density gradients, HT-HUVEC cells were plated on 20 μm wide fibronectin (FN) tracks separated by non-adherent PLL-PEG (described in (*40*)) to force cells to migrate in a linear direction. (**B**) Example gradient quantification during migration on fibronectin stripes. Cells are masked, and then a 3 μm ring inside the cell is analyzed for each normalized biosensor. The distance from the front of the cell is calculated for each pixel in the ring and then binned into 20 equal-length segments. The average value for each bin, on both sides of the cell, is represented in the kymograph along the y-axis. (**C**) Biosensor kymograph of MPAct in RPE-1 migrating on 20 μm FN stripes. RPE-1 stably expressing MPAct-mCitrine and iRFP-CaaX with mean distribution over time shown on the right. Cells were analyzed as in Fig. 2A. (**D**) MPAct signal gradients are time-stable and spatially reproducible. Front-back MPAct/CaaX distribution of single HT-HUVEC stably expressing MPAct-mCitrine and iRFP-CaaX migrating on 20 μm fibronectin stripes from three independent experiments. Time interval for imaging is indicated next to cell. (**E**) Mean MPAct/CaaX distributions for the cells shown in (F) over time. Mean and 95% CI are shown. (**F**) Schematic showing mosaic imaging in HT-HUVEC monolayers. Cells uniformly expressing iRFP-CaaX were transiently transfected with MPAct-mCitrine allowing for sparse labeling (**G**) Example set up of 3D collagen matrix experiment. RPE-1 cells stably expressing MPAct-mCitrine and iRFP-were plated onto an existing collagen gel and then covered with an additional layer of collagen gel and imaged 24 hours later. (**H**) Basal section of randomly migrating HeLa on collagen coated glass transiently transfected with MPAct-mRuby and iRFP-CaaX. (**I**) Basal region of RPE-1 transiently expressing MPAct Ruby and a YPET-membrane randomly migrating on 20 μg/mL fibronectin coated glass. (**J**) TIRF of RPE-1 stably expressing MPAct-mRuby (magenta) and CaaX-anchored sensor (green, as membrane marker) randomly migrating on uniform collagen coated glass. HeLa and RPE-1 showed the same MPA gradient when migrating in 2D on both uniform collagen and fibronectin coated glass. Scale bar = 10 μm unless indicated otherwise. Scale of MPAct/CaaX varies with image modality and cell shape and is normalized to show maximal signal range.

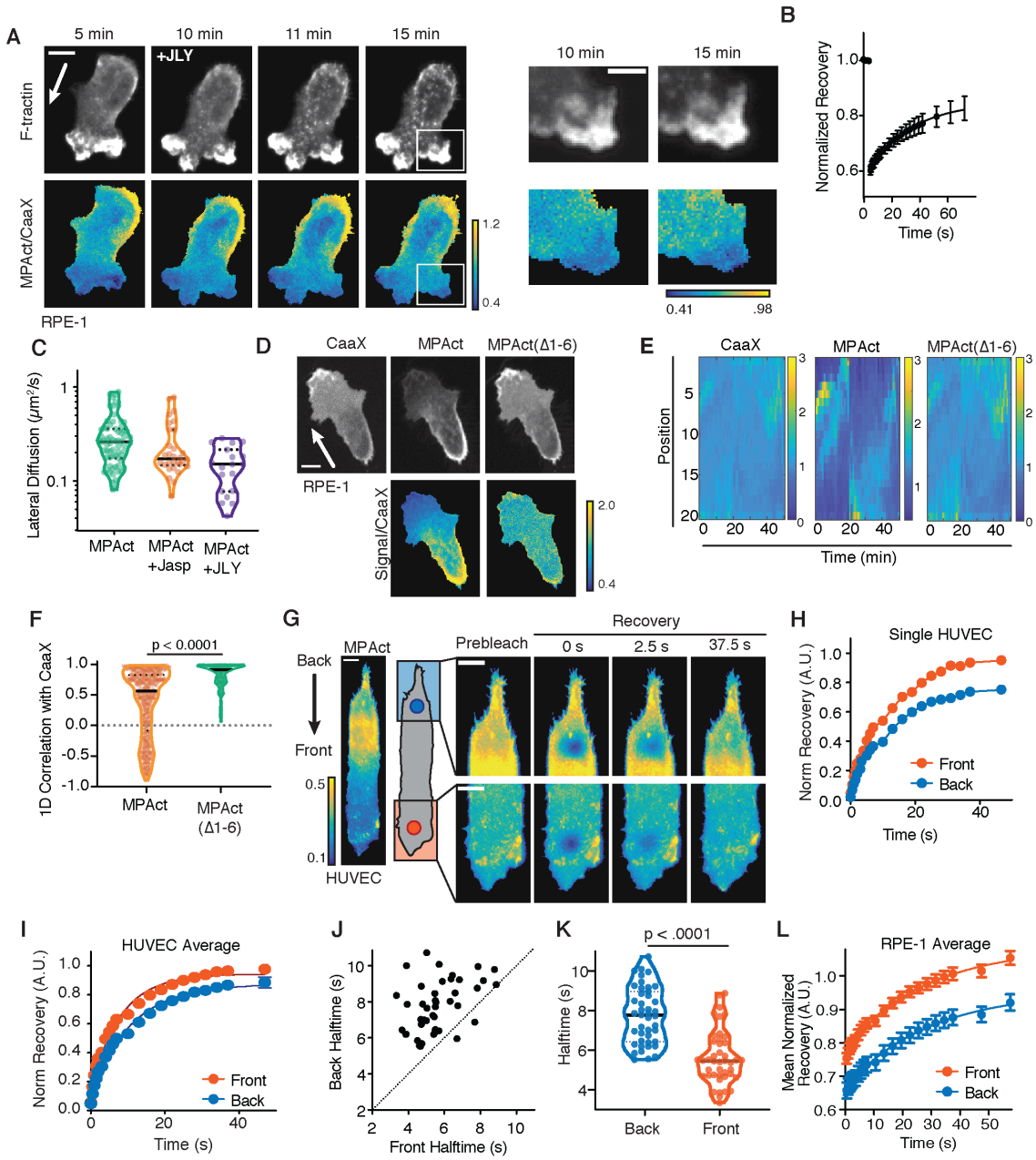
A
5 min
10 min
11 min
15 min
+JLY
F-tractin
MPAct/CaaX
RPE-1
1.2
0.4
10 min
15 min
0.41
.98
B
Normalized Recovery
1.0
0.8
0.6
0 20 40 60
Time (s)
C
Lateral Diffusion (μm²/s)
1
0.1
MPAct
MPAct +Jasp
MPAct +JLY
D
CaaX
MPAct
MPAct(Δ1-6)
RPE-1
Signal/CaaX
2.0
0.4
E
CaaX
MPAct
MPAct(Δ1-6)
Position
5
10
15
20
0 20 40
Time (min)
F
p < 0.0001
1D Correlation with CaaX
1.0
0.5
0.0
-0.5
-1.0
MPAct
MPAct (Δ1-6)
G
Back
MPAct
Prebleach
Recovery
0 s
2.5 s
37.5 s
Front
0.5
0.1
HUVEC
H
Single HUVEC
Norm Recovery (A.U.)
Front
Back
Time (s)
I
HUVEC Average
Norm Recovery (A.U.)
Front
Back
Time (s)
J
Back Halftime (s)
Front Halftime (s)
K
p < .0001
Halftime (s)
Back
Front
L
RPE-1 Average
Mean Normalized Recovery (A.U.)
Front
Back
Time (s)

Fig. S4 MPAct signal gradients result from a reduced binding to MPA in the front compared to the back.

(**A**) MPAct gradients remain in the absence of F-actin turnover and are not a result of limited equilibration of the sensor. RPE-1 cell after treatment with an F-actin-arresting JLY cocktail described in (*42*) and Materials and Methods. F-tractin-mCherry (top) and normalized MPAct-mCitrine/iRFP-CaaX images (bottom) are shown. Two time points for the actin-arrested protrusions are shown at a higher resolution (right). F-tractin enriched protrusions remained stably depleted of MPAct. The stability of the gradient without F-actin dynamics indicates a structural basis for MPAct gradients, that could also be influenced by turnover dynamics. Scale bar = 5 μm. (**B**) MPAct can still laterally diffuse in the JLY treated cells. Average recovery of FRAP of MPAct-mCitrine in the lateral membrane of RPE-1 after 20 min of JLY incubation. N = 22 cells from 1 experiment. Mean and 95% CI are shown. (**C**) Diffusion rates calculated from FRAP experiments preformed on the lateral membrane of RPE-1 based on 2D Gaussian profile fitting for MPAct-mCitrine with 8 μM Jasplakinolide or the JLY cocktail construct n = 69, and 19, 30 respectively from 2 independent experiments. Dotted lines are quartiles. p-values are derived from unpaired t-test. (**D**) MPAct gradients require F-actin binding to form. (Top) Basal section of RPE-1 cells co-expressing CFP-CaaX, MPAct-mCitrine, and MPAct(Δ1-6)-mRuby migrating randomly on collagen coated glass. (Bottom) CaaX normalized MPAct and MPAct(Δ1-6). See Movie S2. (**E**) Control experiments, showing 1D profiles of CFP-CaaX, MPAct-mCitrine, and MPAct(Δ1-6)-mRuby for a RPE-1 cell migrating on uniform collagen. Both CaaX and MPAct(Δ1-6) show a high degree of correlation that is decreased when comparing MPAct and CaaX. The local curvature of the plasma membrane in different regions causes the CaaX membrane marker and MPAct(Δ1-6) to have a similar uneven distribution, while the distribution of the MPAct construct is not correlated with them. **(F)** 1D correlation control analysis of (E) of CaaX with either MPAct or MPAct(Δ1-6). CaaX and MPAct(Δ1-6) are highly correlated (median = 0.91) while CaaX and MPAct show a lower, but positive correlation (median = 0.56). Each point represents a single time-point for a tracked cell. N = 579 total time points for 7 cells. p-values derived from Wilcoxon test. (**G**) MPAct gradients are the result of a relatively lower probability of MPAct binding F-actin in the front based on FRAP analysis. The areas enriched with MPAct sensor should also show a slower recovery if there is more F-actin within the MPAct sensor search radius. Photobleaching recovery analysis of MPAct-mCitrine in HT-HUVEC migrating on 2D fibronectin stripes comparing front versus back. The same area was bleached in both the front and back of the same cell creating paired measurements for MPAct recoveries. (**H**) Example of an individual HT-HUVEC FRAP recovery curves after photobleaching in the front and back from a single cell. (**I**) The back of migrating cells showed slower MPAct recovery than the front of cells. Average recovery curves for the front (red) and back (blue) of cells. N = 48 matched cells pooled from 3 independent experiments. Mean and 95% CI shown. $t_{½}$ = front: 5.48 ± 0.39 s and back: 7.53 ± .605 s, mean ± 95 % CI. (**J**) Half-time recovery rates from individual cells plotted in (I) for direct comparison (N = 48 cells from 3 independent experiments). (**K**) Half-times calculated from individual recovery curves in (I). p-values are from paired t-test. (**L**) Average recovery curves after FRAP for MPAct-mCitrine in the front (red) and back (blue) of RPE-1 migrating randomly on uniform collagen. N = 37 matched cells from 2 independent experiments. Mean and 95% CI

shown. Line of best fit shown fits using 1-phase association is shown for (H,I,L). Scale bar = 10 μm. The relative scale of MPAct/CaaX signals varies with image modality and cell shape and was normalized to show maximal signal range.

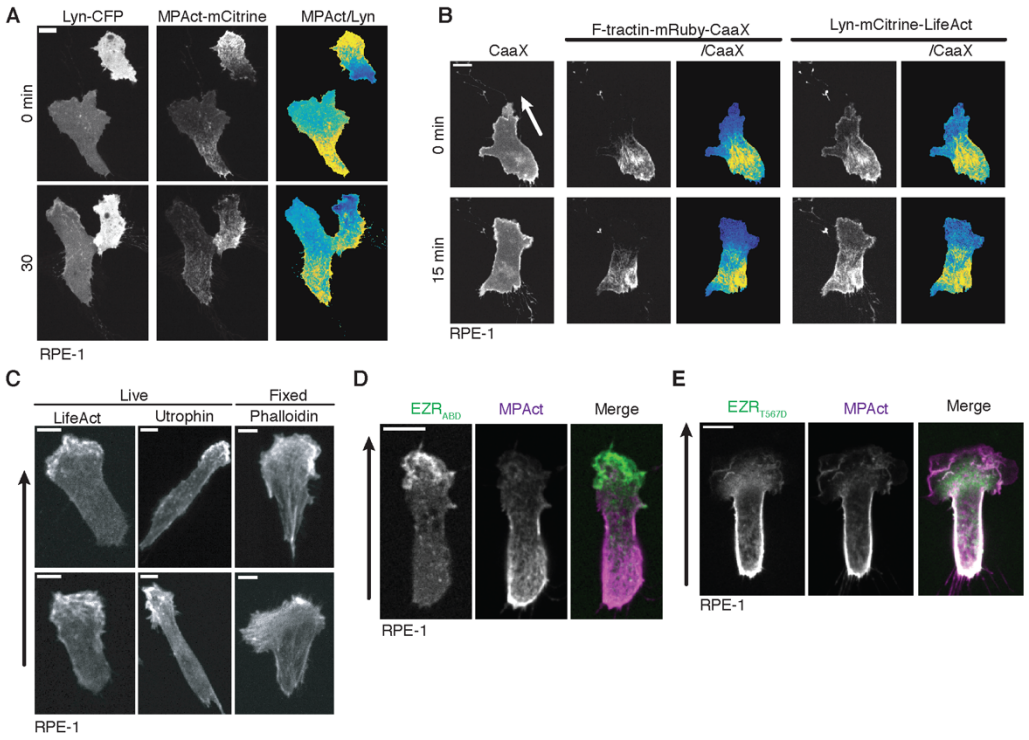
A
Lyn-CFP
MPAct-mCitrine
MPAct/Lyn
0 min
30
RPE-1
B
CaaX
F-tractin-mRuby-CaaX
/CaaX
Lyn-mCitrine-LifeAct
/CaaX
0 min
15 min
RPE-1
C
Live
Fixed
LifeAct
Utrophin
Phalloidin
RPE-1
D
EZR$_{ABD}$
MPAct
Merge
RPE-1
E
EZR$_{T567D}$
MPAct
Merge
RPE-1

Fig. S5 MPAct signal gradients can be recapitulated using variant reporters with different types of membrane anchors, F-actin motifs and normalization methods.

(**A**) MPAct/membrane gradient does not depend on whether a farnesyl-polybasic (CaaX) or a myristoyl-palmitoyl (Lyn_{11}) type membrane anchor was used for the normalization of the reporter. A basal region of randomly migrating RPE-1 expressing Lyn_{11}-CFP (left), a myristoylation and palmitoylation membrane anchor, MPAct-mCitrine (middle) as well as a Lyn-normalized MPAct (right). (**B**) MPAct gradients are not F-tractin/CaaX specific as MPAct variants using different binding motifs show identical gradients. RPE-1 transiently co-expressing WT MPAct (middle) using F-tractin F-actin binding and CaaX membrane association domain and an alternative construct that uses a LifeAct F-actin binding and Lyn_{11} membrane association (right). Both constructs are shown CaaX normalized. (**C**) Most global F-actin sensors are enriched in the front of cells. Randomly migrating RPE-1 transiently expressing LifeAct-GFP(left), GFP-Utrophin-Ch (middle) or fixed and stained with phalloidin (right). F-actin at the front is readily bound by unrelated cytoplasmic actin binding proteins, but the binding is enriched in the back upon tethering to the PM (B,E). Each of the domains tested that showed a gradient (F-tractin, LifeAct, and EZR_{abd}) are expected to bind distinct regions along a F-actin filament. This argues against, but does not eliminate the possibility, of a MPA specific F-actin modification or occlusion that effects all these proteins similarly. (**D-E**) Constructs with similar topology to MPAct (e.g. dual constitutive membrane binding and reversible F-actin binding motifs) all show similar MPA gradients. Constitutively active Ezrin-T567D enriches similar to MPAct (magenta) (D) while the F-actin binding domain of Ezrin ($Ezrin_{abd}$-green) (E) behaves like a normal F-actin probe from (C) (green) and MPAct (magenta). Images from transiently expressed constructs at the basal membrane of migrating RPE-1 cells. Scale bar = 10 μm.

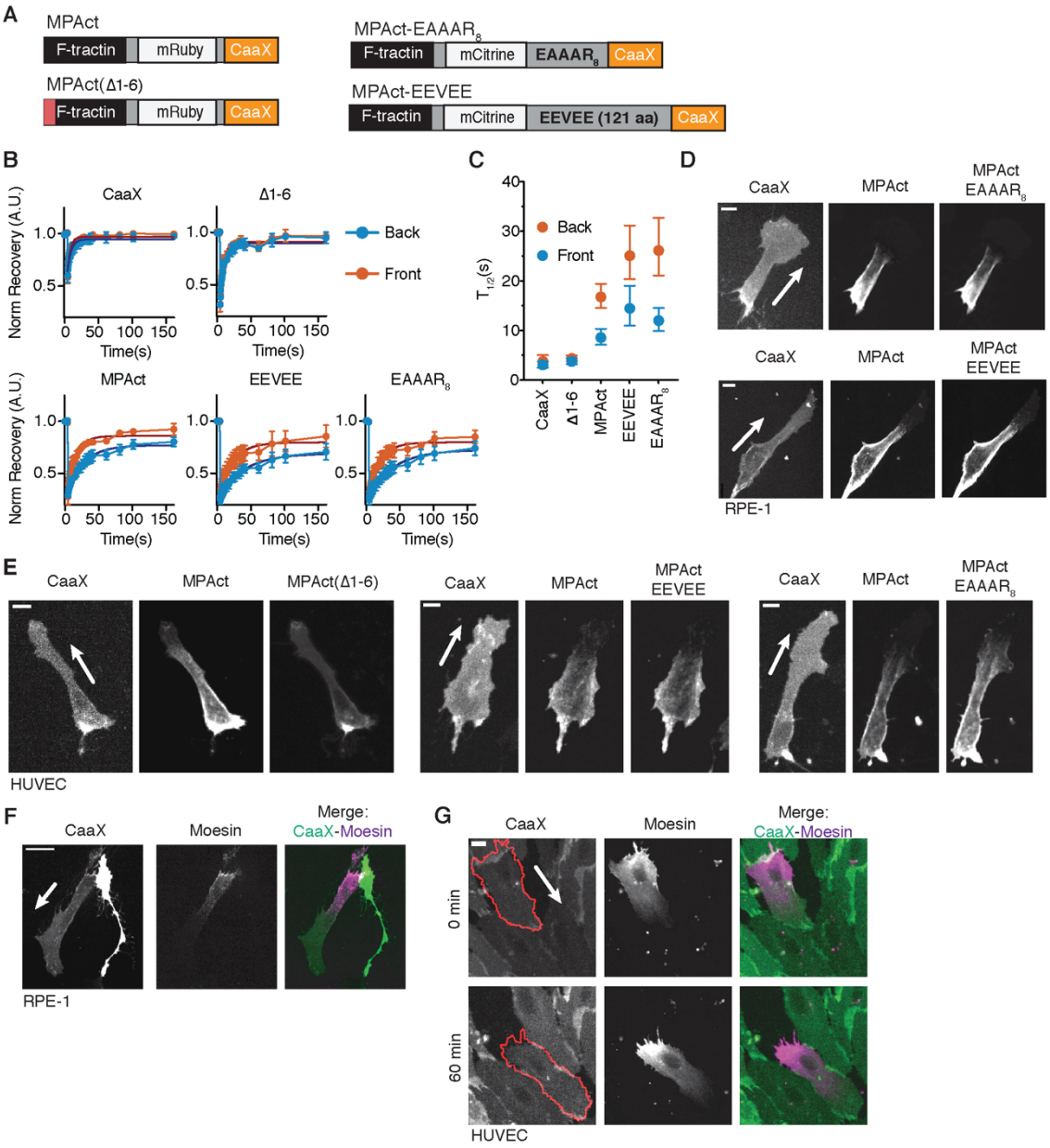
A
MPAct
F-tractin
mRuby
CaaX
MPAct(Δ1-6)
F-tractin
mRuby
CaaX
MPAct-EAAAR8
F-tractin
mCitrine
EAAAR8
CaaX
MPAct-EEVEE
F-tractin
mCitrine
EEVEE (121 aa)
CaaX
B
CaaX
Δ1-6
Norm Recovery (A.U.)
1.0
0.5
0 50 100 150
Time(s)
Back
Front
MPAct
EEVEE
EAAAR8
C
Back
Front
T1/2 (s)
40
30
20
10
0
CaaX
Δ1-6
MPAct
EEVEE
EAAAR8
D
CaaX
MPAct
MPAct EAAAR8
CaaX
MPAct
MPAct EEVEE
RPE-1
E
CaaX
MPAct
MPAct(Δ1-6)
CaaX
MPAct
MPAct EEVEE
CaaX
MPAct
MPAct EAAAR8
HUVEC
F
CaaX
Moesin
Merge:
CaaX-Moesin
RPE-1
G
CaaX
Moesin
Merge:
CaaX-Moesin
0 min
60 min
HUVEC

Fig. S6 Measurements using reporters with different linker length and flexibility argue that the observed MPAct signal gradient is due to local MPA density gradients and not changes in cortex-membrane distance.

(**A**) Schematic of F-actin binding (left) and linker length (right) variants constructed for this study. MPAct(Δ1-6) uses a F-tractin(Δ1-6) instead of full-length F-tractin, which showed no F-actin binding. MPAct-$(EAAAR)_8$ ((*43*) right-top), inserts a 40 a.a. rigid helix in between the fluorescent protein and the CaaX. MPAct-EEVEE ((*19*) right-bottom), inserts a 121 a.a. flexible linker from the Raichu family of FRET biosensors in between the fluorescent protein and the CaaX. The $(EAAAR)_8$ and EEVEE variants can be used to test if different local distances or orientations of F-actin filaments of MPA from the plasma membrane are responsible for the observed MPAct gradients. (**B**) Recovery curves after photobleaching in the front and back of randomly migrating RPE-1 cells transiently expressing various MPAct or control constructs as indicated. Each cell was bleached twice (similar to Fig. S4E) $N \geq 6$ cells per construct. (**C**) Increasing MPAct "search radius" does not change the relatively slower $T_{1/2}$ recovery in the back compared to the front. Increasing the tether range of the reporter increased the $T_{1/2}$ both in the front and back showing a higher accessibility to F-actin with increased $T_{1/2}$ times for recovery after photobleaching for each construct shown in (E) in the front and back of cells. $T_{1/2}$ calculated from a one-phase association using GraphPad Prism 8. (**D**) MPAct linker variants showed identical gradients despite increased search radius and angular flexibility suggesting MPAct gradient results from differences in the averaged local membrane-proximal F-actin density. Basal section of RPE-1 cells co-expressing iRFP-CaaX, MPAct-mRuby3, and either MPAct-$(EAAAR)_8$-mCitrine (top) or MPAct-EEVEE-mCitrine (bottom) migrating randomly on collagen coated glass. (**E**) Basal section of HT-HUVEC monolayers transiently transfected with MPAct (Δ1-6)-mRuby (left), MPAct-EEVEE-mCitrine (middle) and MPAct-$EAAAR_8$-mCitrine (right) along with the WT MPAct-mCitrine or mRuby and CFP-CaaX. For all images direction of migration is indicated by the white arrow. Scale bar is 10 μm. (**F**) Monolayers expressing iRFP-CaaX (left, green) transiently transfected with GFP-moesin (middle, magenta). Cell outline in the monolayer is shown in red. (**G**) Basal section of iRFP-CaaX(left, green) and GFP-moesin (middle, magenta) transiently co-expressed in randomly migrating RPE-1 cells. Exogenously tagged Moesin showed a similar enrichment to the back of migrating cells. Direction of migration indicated with an arrow. Scale bar = 10 μm.

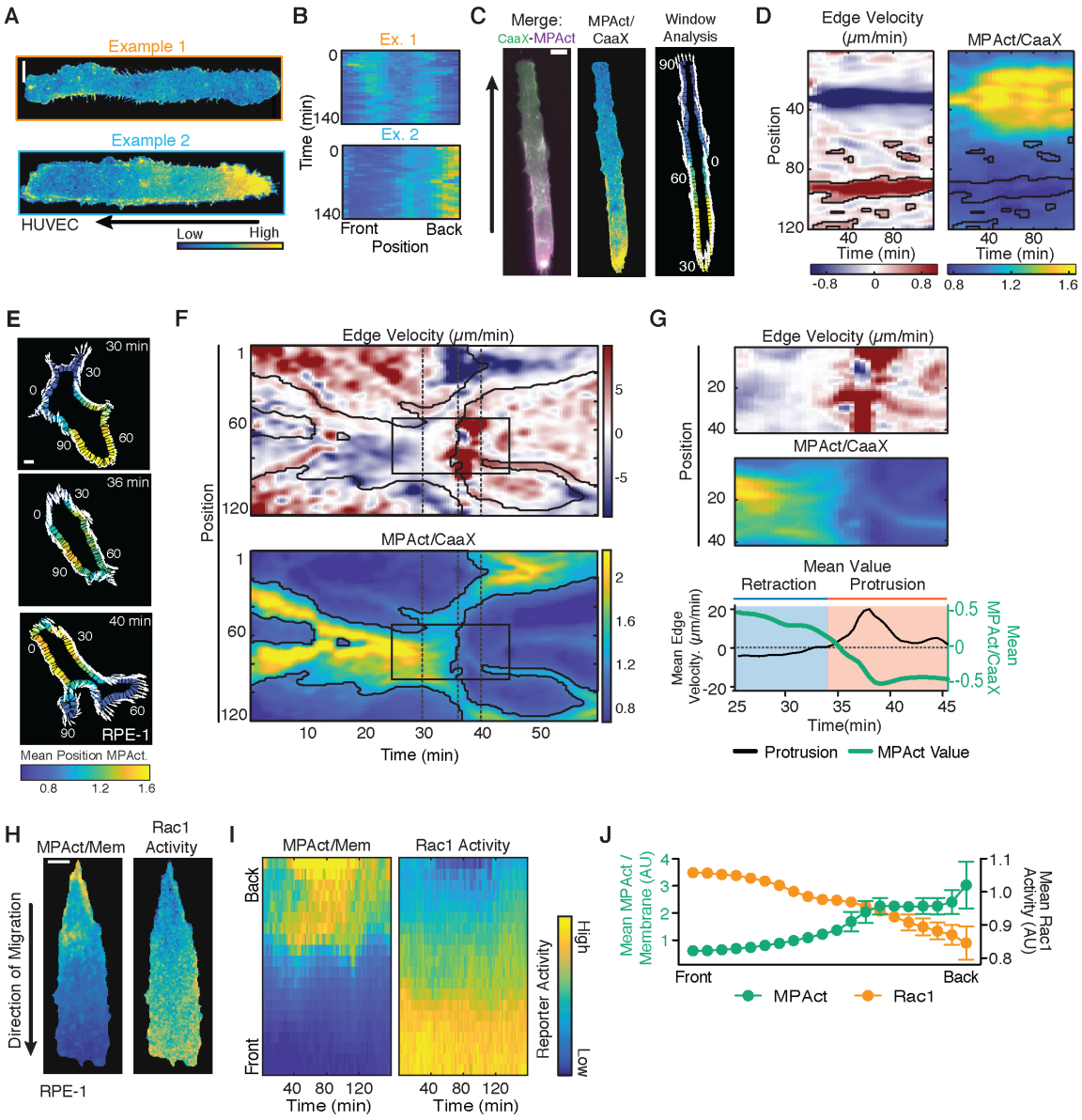
A
Example 1
Example 2
HUVEC
Low
High
B
Ex. 1
Ex. 2
Time (min)
Front
Back
Position
C
Merge:
CaaX-MPAct
MPAct/
CaaX
Window
Analysis
D
Edge Velocity
(μm/min)
MPAct/CaaX
Position
Time (min)
E
30 min
36 min
40 min
RPE-1
Mean Position MPAct.
F
Edge Velocity (μm/min)
MPAct/CaaX
Position
Time (min)
G
Edge Velocity (μm/min)
MPAct/CaaX
Position
Mean Value
Retraction
Protrusion
Mean Edge
Velocity (μm/min)
Mean
MPAct/CaaX
Time(min)
Protrusion
MPAct Value
H
MPAct/Mem
Rac1
Activity
Direction of Migration
RPE-1
I
MPAct/Mem
Rac1 Activity
Back
Front
Reporter Activity
High
Low
Time (min)
J
Mean MPAct /
Membrane (AU)
Mean Rac1
Activity (AU)
Front
Back
MPAct
Rac1

Fig. S7 Sites of low MPA density are permissive for local membrane protrusion. (**A, B**) Representative cells from Fig. 3C,D shown as two images (A) and kymographs (B). Analysis identical to Fig. S3A. Cells were tracked for > 140 min and imaged every 2 min. (**C**) Edge velocity window analysis for HT-HUVEC expressing CFP-CaaX and MPAct-mCitrine migrating on 20 μm FN stripes. Analysis pipeline was identical to that used in Fig. 3E-F. Merge (left) and MPAct /CaaX (middle) are shown. For each window mean MPAct/CaaX (right) is indicated by the color of the region and edge velocity in the following frame is indicated by the direction and length of the white arrow emanating from that window. (**D**) Window analysis for edge velocity (left) and MPAct/CaaX (right) for the cell in (C). Window number (y-axis) vs Time (x-axis) pseudo-colored to show protrusive areas (red) and retracting areas (blue) for protrusion and retraction, or with parula for the MPAct/CaaX. (**E-G**) Example edge correlation and protrusion alignment analysis for a repolarizing RPE-1 cell. Window parameterization for the time points indicated by the dotted lines shown in (E). Example timepoints showing MPAct/CaaX window parametrization and edge velocity (white arrows) for a cell changing direction. For each window mean MPAct is indicated by the color of the region and displacement in the following frame is indicated by the direction and length of the white arrow emanating from that window. (F) Edge correlation analysis for the cell in (E) showing edge velocity (above) and MPAct/CaaX (below). The 3 dashed vertical line show the time points shown in (E). Black box shows repolarization event that is examined more closely in (G). (G) Kinetics of protrusion and MPAct changes during repolarization. Semi-automatic analysis of edge velocity maps selected the windows and timing of each polarization event. Edge velocity (top) and MPAct/CaaX ratio (middle) for that region. Bottom shows average values for each vs time. Protrusion is shown in black (left y-axis) and MPAct is shown in green (right y-axis). (**H**) RPE-1 stably co-expressing MPAct-mRuby (Left) and Raichu-Rac1 FRET sensor were plated onto 20 μm fibronectin stripes and imaged using simultaneous confocal imaging. Resulting normalized intensities are shown for a single time point. (**I, J**) Activity profile of MPAct/membrane and Rac1 activity (I) and mean distribution over time (J) for Rac1 activity (black, right y-axis) and MPAct/Membrane (green, left y-axis) for the cell shown in (H) over 160 min. Scale bar = 10 μm.

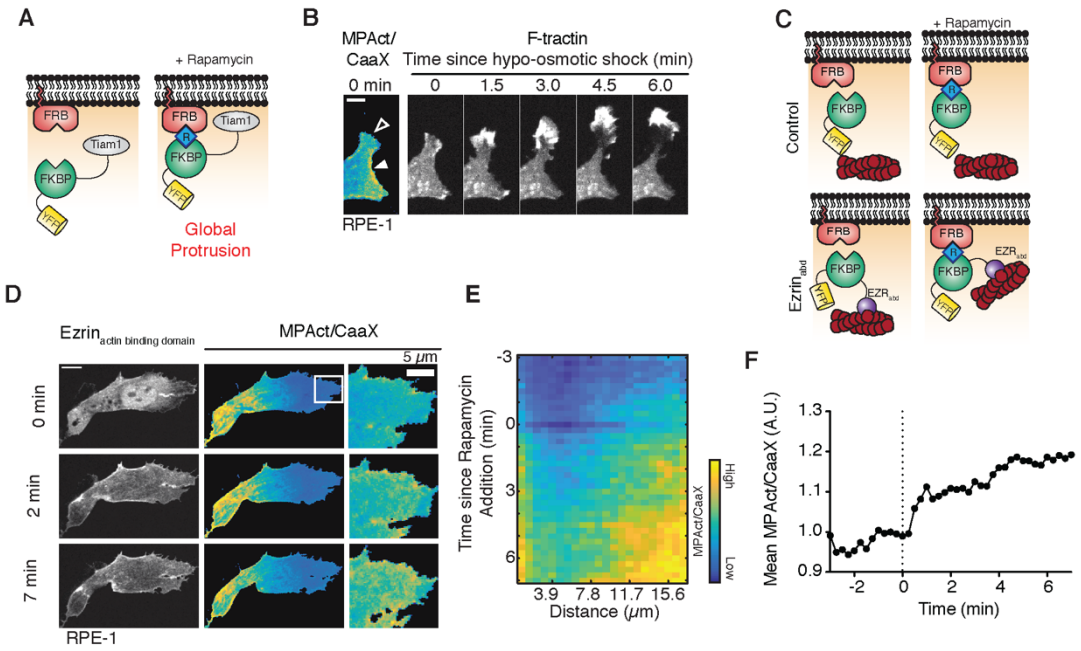

Fig. S8 Locally low MPA density directs osmotically driven membrane protrusions and inhibits existing protrusion

(**A**) Schematic of Tiam1-FKBP/Lyn-FRB Rac activation system. FKBP tagged Tiam1 has cytoplasmic localization until addition of the small molecule rapamycin. Rapamycin induced dimerization with the membrane anchored Lyn_{11}-FRB recruits Tiam1 to the membrane uniformly where it can induce cell-wide protrusion. (**B**) (left) MPAct/CaaX shown for a basal membrane of RPE-1 prior to hypo-osmotic shock with 100 µL ddH_2O. (Right) evolution of protrusion after osmotic shock based on F-tractin. (**C**) Schematic for a FKBP-FRB construct to acutely increase membrane proximal F-actin compared to a control construct. Recruitment of the $Ezrin_{abd}$ to the plasma membrane should both increase membrane tethering and promote de novo cortex polymerization (*37*) and cause an increase in MPA. (**D**) Change in MPAct-mRuby enrichment after FKBP-EZR_{abd} is recruited to the membrane following addition of 5 µM rapamycin. Area shown in white box in the left is shown at higher resolution with a different color scale to highlight difference over time. (**E**) Kymograph of the MPAct-mCitrine intensity from the inset area in (D) over time (horizontal axis). (**F**) Quantification of a mean MPAct-mRuby fluorescence in a protrusive area after recruitment of FKBP-EZR_{abd} to the membrane. Scale bar = 10 µm.

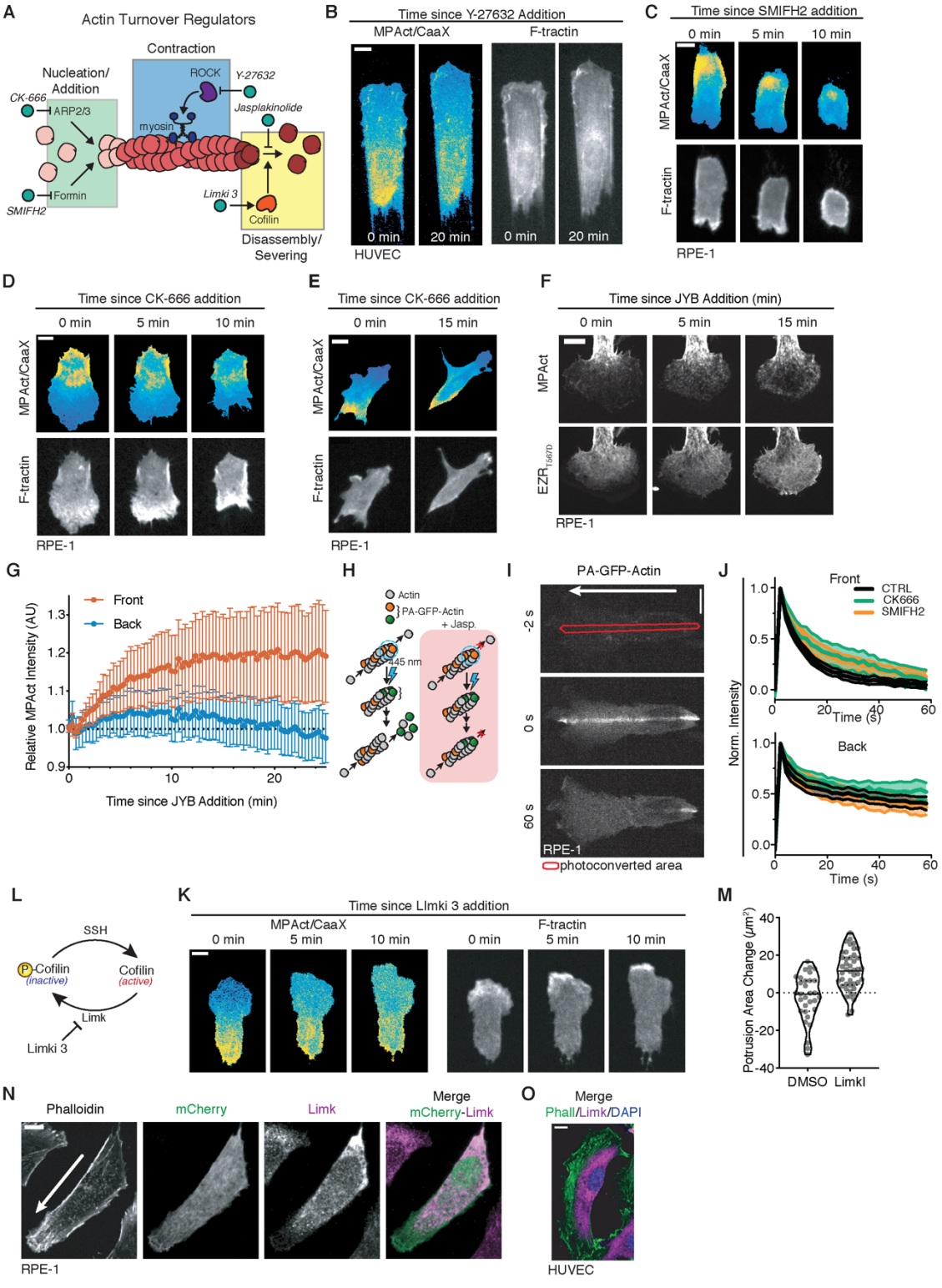
A
Actin Turnover Regulators
Contraction
Nucleation/
Addition
ROCK
Y-27632
CK-666
ARP2/3
myosin
Jasplakinolide
Formin
SMIFH2
Limki 3
Cofilin
Disassembly/
Severing
B
Time since Y-27632 Addition
MPAct/CaaX
F-tractin
0 min
20 min
0 min
20 min
HUVEC
C
Time since SMIFH2 addition
0 min
5 min
10 min
MPAct/CaaX
F-tractin
RPE-1
D
Time since CK-666 addition
0 min
5 min
10 min
MPAct/CaaX
F-tractin
RPE-1
E
Time since CK-666 addition
0 min
15 min
MPAct/CaaX
F-tractin
RPE-1
F
Time since JYB Addition (min)
0 min
5 min
15 min
MPAct
EZR T567D
RPE-1
G
Front
Back
Relative MPAct Intensity (AU)
1.3
1.2
1.1
1.0
0.9
0
10
20
Time since JYB Addition (min)
H
Actin
PA-GFP-Actin
+ Jasp.
445 nm
I
PA-GFP-Actin
-2 s
0 s
60 s
RPE-1
photoconverted area
J
Front
CTRL
CK666
SMIFH2
1.0
0.5
0.0
0
20
40
60
Time (s)
Norm. Intensity
Back
1.0
0.5
0.0
0
20
40
60
Time (s)
L
SSH
P Cofilin
(inactive)
Cofilin
(active)
Limk
Limki 3
K
Time since LImki 3 addition
MPAct/CaaX
F-tractin
0 min
5 min
10 min
0 min
5 min
10 min
M
Potrusion Area Change (μm²)
40
20
0
-20
-40
DMSO
LimkI
N
Phalloidin
mCherry
Limk
Merge
mCherry-Limk
RPE-1
O
Merge
Phall/Limk/DAPI
HUVEC

Fig. S9 High cofilin activity and actin disassembly rates in the front establish the gradient in MPA density during cell migration.

(**A**) Local F-actin density near the surface membrane could be controlled by several regulatory processes: F-actin disassembly, polymerization, or actomyosin contraction. Schematic of actin turnover showing monomer addition at the + end (green box) highlighting the roles of Arp2/3 and formins, contraction by myosin motors (blue box) and filament disassembly and severing (yellow box) by cofilin and possibly other proteins. Specific drug perturbations to these processes are shown as teal circle with the associated drug name. These drugs were tested to see if MPAct localization changes could occur before the overall polarity of F-actin changes. (**B**) Treatment with Y-27632 caused a gradual loss of cell polarity paralleled by an equally slow loss of the MPAct signal gradient, suggesting that myosin contraction does not directly regulate the MPA density gradient. MPAct/CaaX and F-tractin for HT-HUVEC migrating on 20 μm FN stripe before and after treatment with 10 μM Y-27632. (**C, D**) Inhibition of the formin regulators of actin nucleation and polymerization with the drug SMIFH-2 or the actin nucleator Arp2/3 with CK-666 caused gradual and parallel loss of cell polarity and MPAct signal gradients (Example images from basal section for RPE-1treated with 20 μM SMIFH2 (C) and 100 μM CK-666 (D)). Cells transiently co-expressed MPAct/CaaX (top) and F-tractin (bottom). (**E**) Cell that maintained polarization after CK-666 treatment show thin filopodia like protrusions (F-tractin-bottom) emanating from previous areas of broad protrusions while maintaining MPAct polarity (top). (**F**) Loss of the MPA density gradient and increased EZR_{T567D} localization to the front of migrating cells in response to JYB addition. This result differs from the experiments where we also blocked F-actin polymerization using a JLY cocktail where the MPAct signal gradient remains stable (Fig. S4A). Example images from the from the front of RPE-1 cell transiently co-expressing GFP-EZR_{T56D}, MPAct-mRuby, and iRFP-CaaX before and after treatment with JYB cocktail. (**G**) MPAct increases in the front of cells more than the back under inhibition of F-actin severing. Average MPAct increase in the front (red) and back (blue) of migrating cells after JYB cocktail addition. Values are normalized to the average value for the 5 frames prior to drug addition. N = 24 cells, mean ± 95% CI are shown. **(H)** Schematic of actin turnover analysis using photoconvertible PA-GFP-actin, without (left) and with (right) stabilization by Jasplakinolide. (**I**) Example of PA-actin-GFP photoconversion in an RPE-1 cell. The outlined area shows where the photoconversion occurred. All frames are shown with the same color scale to show dynamic range of photoconversion. (**J**) GFP-actin fluorescence was lost faster in the front compared to the back even after treatment with the actin nucleation inhibitors SMIFH2 and CK-666. Mean PA-GFP-Actin fluorescence loss at the front (left) and back (right) of migrating RPE-1 without (black, N = 24 cells) and with 100 μM CK-666 (green, N = 16 cells), or 20 μM SMIFH2 (orange, N = 20 cells). Mean and 95% CI are shown. **(K)** Schematic of cofilin activation cycle by SSH and inactivation Limk. (**L**) Example images from basal section (right) for RPE-1treated with 20 μM Limki 3. Cells co-expressed MPAct/CaaX (left) and F-tractin (right). **(M)** Protrusion area change 5 min after DMSO or Limki 3 addition. N = 31,44 cells. (**N**) Immunofluorescence of WT RPE-1 cells after transient transfection with mCherry as a cytoplasmic marker. Cells were subsequently fixed and stained with endogenous Limk and phalloidin to ensure localization of Limk was not reflective of general cytoplasm asymmetries. (**O**) HT-HUVEC stained with phalloidin,

anti-αLimk antibody, and Hoechst. Images were background subtracted before ratio and measurements. For all images direction of cell migration is indicated by a white arrow on the CaaX image or by the black arrow to the left of the cell. Scale bar = 10 μm unless otherwise noted.

Movie S1

Ratio of MPAct-mCitrine/iRFP-CaaX in a HT-HUVEC cell migrating on 20 μm fibronectin stripes shown in parula color scale. 3 cells shown are from independent experiments. Scale bar = 10 μm.

Movie S2

Normalized MPAct-mRuby3/iRFP-CaaX (left) and MPAct-(Δ1-6)-mCitrine/iRFP-CaaX (right) in the same RPE-1 cell. Shown cell is randomly migrating on uniform collagen coated glass plates. Scale bar = 10 μm.

Movie S3

Normalized MPAct-mRuby3/iRFP-CaaX and SSH/Limk (left) after LIMKi 3 addition. Shown RPE-1 cell is randomly migrating on uniform collagen coated glass plates. Scale bar = 10 μm.